Electric permittivity and dynamic mobility of dilute suspensions of plate-like gibbsite particles

M. Alejandro González, Ángel V. Delgado, Raúl A. Rica[1]*, María L. Jiménez, Silvia Ahualli*[*]

Supplementary Information

1. Comparison of electrophoretic mobility calculations for spheres and spheroids

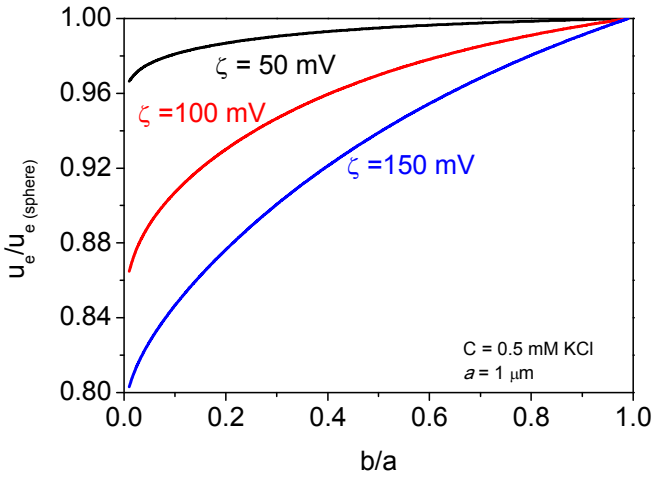

Figure S1. Electrophoretic mobility of oblate spheroids as a function of axial ratio for the indicated zeta potentials, relative to that of spheres with radius *a*, calculated with the O'Brien and Ward model.[1]

[1]Present address: ICFO-Institut de CiènciesFotòniques, 08660 Castelldefels, Barcelona, Spain.

2. Polarization of the electrical double layer

2.1.The dipole moment

Although the dispersed particles and their EDLs will most likely be apolar, that is, will lack a permanent dipole moment, this can be induced by the field. A linear response is assumed, and hence the nucleus of our discussion is the dipole coefficient C_0^*, a complex quantity relating the induced dipole moment $d^* \exp(-j\omega t)$ to the external field, which will be assumed harmonic, with frequency ω, $E_{ext} = E \exp(-j\omega t)$. The same frequency dependence will apply to all quantities, and hence we will avoid the repeated use of the exponential term. If V_p is the particle volume, the relationship between the dipole moment and the dipole coefficient is:

$$\begin{aligned} d^* &= 3V_p C_0^* E \\ C_0^*(\omega) &= C_1(\omega) - jC_2(\omega) \end{aligned} \qquad \text{[S.1]}$$

The complex dipole coefficient has been expressed in terms of its real and imaginary components, C_1 and C_2, respectively.

2.2.Consequences. Dielectric relaxation

The importance of the dipole coefficient can be understood first of all by considering how it determines the frequency dispersion of the permittivity of the suspension, typically expressed in terms of the relative permittivity (or dielectric constant) and the permittivity of vacuum: $\varepsilon^*(\omega)\varepsilon_0$. Because there is no way of directly determining the permittivity, it is of interest to relate it to the complex conductivity $K^*(\omega)$, of easier experimental access, because it can be obtained from impedance $Z^*(\omega)$ measurements of samples using calibrated conductivity cells:

$$K^*(\omega) = \frac{\lambda}{Z^*(\omega)} \qquad [S.2]$$

whereλ is the cell constant. The relationship between both quantities is:

$$\begin{gathered} K^*(\omega) = K_{DC} + j\omega\varepsilon_0\varepsilon^*(\omega) \\ \varepsilon^*(\omega) = \varepsilon'(\omega) - j\varepsilon''(\omega) \\ K^*(\omega) = K_{DC} + \omega\varepsilon_0\varepsilon''(\omega) + j\omega\varepsilon_0\varepsilon'(\omega) \end{gathered} \qquad [S.3]$$

where K_{DC} is the electrical conductivity of the suspension at constant (dc) field. Using eq [S.3]:

$$\begin{gathered} \varepsilon'(\omega) = \frac{\mathrm{Im}\left[K^*(\omega)\right]}{\omega\varepsilon_0} \\ \varepsilon''(\omega) = \frac{\mathrm{Re}\left[K^*(\omega)\right] - \mathrm{Re}\left[K^*(\omega \to 0)\right]}{\omega\varepsilon_0} \end{gathered} \qquad [S.4]$$

Maxwell and Wagner independently obtained a mixture formula relating the conductivity to the dipole coefficient of individual particles[2], for cases where the volume fraction of solids, ϕ, is low:

$$K^*(\omega) = K_m^*(\omega)\left(1 + 3\phi C_0^*(\omega)\right) \qquad [S.5]$$

where K_m^* is the complex conductivity of the medium (the dispersing liquid without particles) which, assuming that the frequency range of interest does not involve any relaxation in the polarization of such medium (its relative permittivity ε_m is constant), can be written $K_m^* = K_m + j\omega\varepsilon_0\varepsilon_m$. Using equations [S.4] and [S.5], the fundamental relationships between the permittivity and the dipole coefficient components are clear:

$$\varepsilon'(\omega) = \varepsilon_m + 3\phi\varepsilon_m\left[C_1(\omega) + \frac{K_m}{\omega\varepsilon_m}C_2(\omega)\right]$$
$$\varepsilon''(\omega) = 3\phi\varepsilon_m C_2(\omega) + \frac{3\phi K_m}{\omega}\left[C_1(\omega) - C_1(\omega = 0)\right] \qquad [S.6]$$

It is common to use incremental quantities to highlight the weight of the particles in the average permittivity. Dielectric increments (both relative to the vacuum permittivity), total and specific, will be denoted $\Delta\varepsilon^*(\omega) = \Delta\varepsilon'(\omega) - j\Delta\varepsilon''(\omega)$ and $\delta\varepsilon^*(\omega) = \delta\varepsilon'(\omega) - j\delta\varepsilon''(\omega)$ respectively:

$$\varepsilon'(\omega) = \varepsilon_m + \varepsilon_0\Delta\varepsilon'(\omega) = \varepsilon_m + \varepsilon_0\phi\delta\varepsilon'(\omega)$$
$$\varepsilon''(\omega) = \varepsilon_0\Delta\varepsilon''(\omega) = \varepsilon_0\phi\delta\varepsilon''(\omega) \qquad [S.7]$$

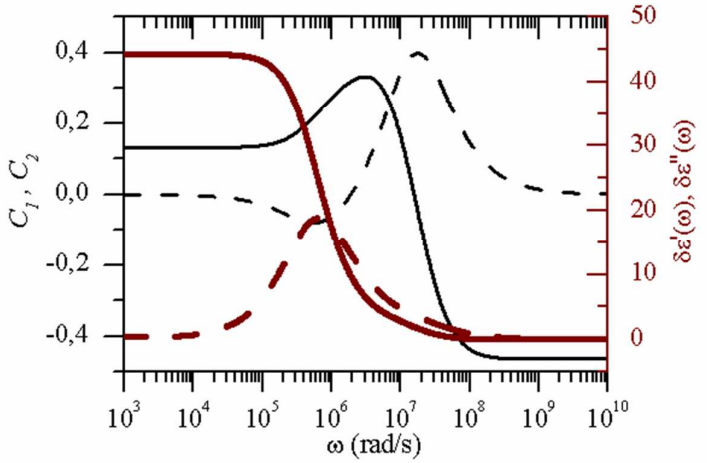

Figure S2. Left (black, thin lines): frequency dependence of the real (solid line) and imaginary (dashed line) components of the induced dipole coefficient of latex spheres (5% v/v) 100 nm in diameter in 0.5 mMKCl solutions, for the zeta potential 100 mV. Right (brown, thick lines): real (solid line) and imaginary (dashed line) components of

the specific dielectric increment calculated from the dipole coefficient for the same frequency interval.

Figure S2 illustrates the relationship between the dielectric and dipole coefficient frequency dispersions. The main finding is that the low frequency permittivity undergoes a significant relaxation in the few-kHz frequency range, also present in the induced dipole moment: this is the alpha-relaxation, with frequency ω_α, well described by Dukhin and Shilov[3,4] At still higher frequencies, the Maxwell-Wagner or Maxwell-Wagner-O'Konski relaxation is observable (although not always: its amplitude is much lower than that of the concentration-polarization). The values of the corresponding relaxation frequencies read:[2,4]

$$\omega_\alpha = \frac{2D_{eff}}{a^2}$$
$$\omega_{MWO} = \frac{K_p + 2K_m}{\varepsilon_0\left(\varepsilon_p + 2\varepsilon_m\right)} \qquad \text{[S.8]}$$

where $D_{eff} = D^+D^-/\left(D^+ + D^-\right)$ for a 1-1 electrolyte solution, ε_p is the dielectric constant of the particle, and the particle conductivity K_p is mainly associated to its EDL through the surface conductivity K^σ. For a spherical particle[5]:

$$K_p = \frac{2K^\sigma}{a} \qquad \text{[S.9]}$$

These frequencies are determinant of the dielectric spectra. A physical feeling of the different polarization behaviors of the EDL in the various frequency ranges considered can be acquired by noting the limiting values of C_0^* for the frequencies mentioned. An approximate expression for the coefficient can be given as follows:

$$C_0^* = \frac{\varepsilon_p^* - \varepsilon_m^*}{\varepsilon_p^* + 2\varepsilon_m^*}$$
$$\varepsilon_{p,m}^* = \varepsilon_{p,m} - j\frac{K_{p,m}}{\omega\varepsilon_0} \qquad [S.10]$$

where K_i is the conductivity of the material. As can be seen, at high frequencies it is the permittivity mismatch that matters, and C_0 tends to -1/2 if the permittivity of the medium is much greater than the particle:

$$C_0(\omega \to \infty) = \frac{\varepsilon_p - \varepsilon_m}{\varepsilon_p + 2\varepsilon_m} \approx -\frac{1}{2} \qquad [S.11]$$

Conversely, at low frequencies the polarization is controlled by the conductivity balance. If, as in our case, the particle is non-conductive, equation [S.10] can still be used, provided that, according to the model proposed by O'Konski (see Ref.[2,6]), the particle, even if insulating, is assigned an effective bulk conductivity because of the (excess) surface conductivity of its double layer. It has become traditional to use the dimensionless Dukhin number, *Du,* for specifying the role of that surface conductivity, K^σ, on the electrokinetics of the system[5]:

$$C_0 = \frac{2Du - 1}{2Du + 2}$$
$$Du = \frac{K^\sigma}{aK_m} \qquad [S.12]$$

2.4.Consequences. Electrophoresis in ac fields

The role of EDL polarization on the electrophoretic mobility of a dispersed particle has been considered carefully since the pioneering works of Overbeek[5,7]: a very

simple model, actually valid for dc fields and thin EDL[4], leads to the following relationship between the mobility u_e and the zeta potential ζ:

$$u_e = \frac{2}{3}\frac{\varepsilon_m}{\mu_m}(1 - C_0)\zeta \qquad [S.13]$$

From equation [S.12] it follows that if the zeta potential is small (hence also K^σ and *Du*), the dipole coefficient takes the value -1/2. Equation [S.13] therefore leads to Helmholtz-Smoluchowski mobility formula $\left(u_e = \frac{\varepsilon_m}{\mu_m}\zeta\right)$. Conversely, for high zeta potential $C_0 \to 1$, which would mean a null value of mobility, precisely when the charge of the particle is high. This paradox is resolved by considering the role of EDL polarization on C_0, above discussed. In fact, as shown in Figure S2, the dipole coefficient does not reach the value of +1. This is because of the occurrence of EDL polarization (concentration polarization) reduces the strength of the induced dipole moment by producing diffusive fluxes of counterions compensating for the field-induced accumulation. This is the reason why the mobility does not increase indefinitely with ζ, but it rather reaches a plateau, as shown in the now classical results of O'Brien and White.[8] Although qualitatively, the approximate equation [S.13] can provide clues regarding the effect of the field frequency on the electrophoretic mobility when an alternating electric field is applied to the suspension, a subject which has been investigated extensively in latest years[9-14]. Figure S3 illustrates the expected behavior of the real and imaginary components of the (complex) frequency-dependent mobility (dynamic mobility), obtained based on the model described in Ref.[15]

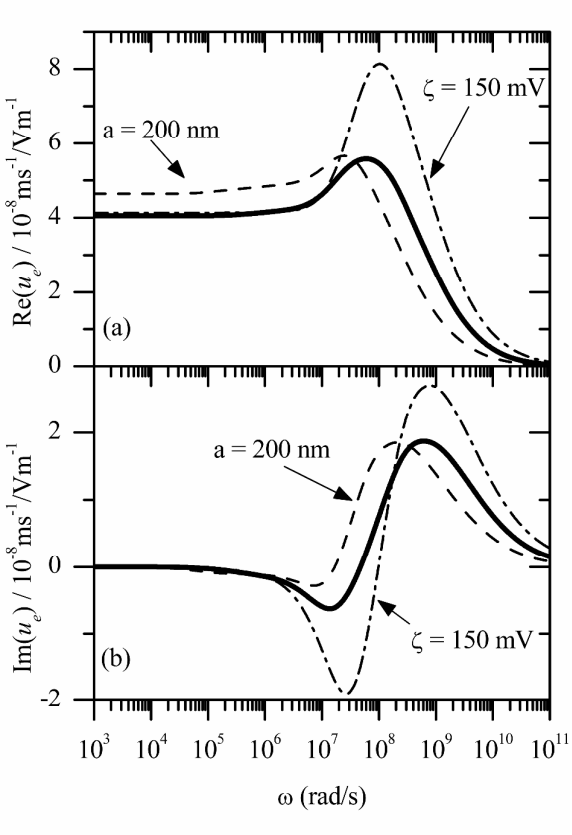

Figure S3. Frequency dependence of the real (a) and imaginary (b) components of the dynamic mobility of latex spherical particles 100 nm in radius and diffeerent zeta potentials; ζ = 100 mV is considered. The ionic strength is 0.5 mMKCl in all cases. The other lines correspond to the same parameter values, except for the one indicated by the label in each case.

Note how the two relaxations associated to the dipole coefficient are observable in the mobility spectrum. The alpha relaxation produces an increase in the real part of the coefficient when the frequency raises above ω_α, and this manifests in a reduction of $Re[u_e]$; in addition the MWO relaxation brings about an increase in the mobility associated to the corresponding decline in the dipole coefficient. There is still a final

relaxation related to the time it takes to set up the movement of fluid and particle. Under the action of the electric field, the liquid in the area of the double layer is moved over the surface of the particle almost instantaneously. However, outside it, at a distance of the order of the radius of the particle, the fluid takes a time to reach its steady state hydrodynamic profile. This characteristic time is of the order of:[16]

$$\tau_h = O\left(\frac{a^2 \rho_m}{\eta_m}\right) \qquad \text{[S.14]}$$

For the case of a = 100 nm particles suspended in aqueous solution $\tau_h = O\left(10^{-8} s\right)$. The frequency associated with these processes is therefore about tens of MHz, and above this characteristic value the electrophoretic mobility decreases drastically because neither the particle nor the fluid can now follow the oscillations of the field (inertial relaxation).

3. The case of spheroidal particles

3.1. Electric permittivity of the suspensions

In the case of oblate spheroidal particles, the first step is the modification of eq [S.1]. For a reference system like the one in Figure S4, we write:

$$d_i^*(\omega) = 4\pi\varepsilon_0\varepsilon_m ab^2 C_i^*(\omega) E_i, \quad i \equiv \square, \perp \qquad \text{[S.15]}$$

corresponding to directions parallel and perpendicular, respectively, to the symmetry axis of the particle. For an arbitrary orientation θ with respect to the field, one has:

$$\mathbf{d}^* = 4\pi ab^2 \varepsilon_0 \varepsilon_m E\left(C_{\square}^* \cos\theta \hat{\mathbf{e}}_{\square} + C_{\perp}^* \cos\theta \hat{\mathbf{e}}_{\perp}\right) \qquad \text{[S.16]}$$

where $\left(\hat{\mathbf{e}}_{\square}, \hat{\mathbf{e}}_{\perp}\right)$ are unit vectors parallel and perpendicular to the symmetry axis.

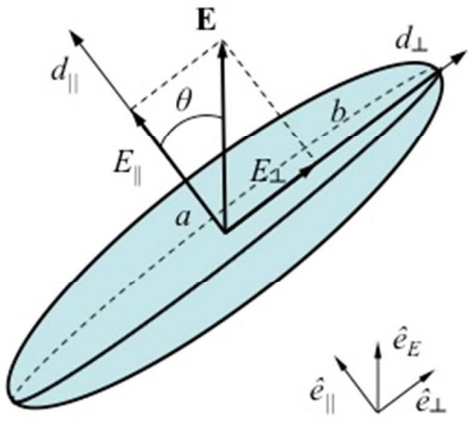

Figure S4: Spheroid semiaxes and components of the dipole and the field.

Like in the case of spherical particles, knowledge of the two complex dipole coefficients $C_{\square}^*, C_{\perp}^*$ allows the prediction of both the dielectric spectrum and the dynamic mobility of the suspension. In particular, for the evaluation of either conductivity or permittivity all that is needed is the component of $\mathbf{d}^*$ parallel to the field:

$$d_E^* = 4\pi ab^2 \varepsilon_0 \varepsilon_m E\left(C_{\perp}^* + \left(C_{\square}^* - C_{\perp}^*\right)\cos^2\theta\right) \qquad [S.17]$$

and its average for random orientation:

$$\left\langle d_E^* \right\rangle = 4\pi ab^2 \varepsilon_0 \varepsilon_m E \frac{2C_{\perp}^* + C_{\square}^*}{3} \qquad [S.18]$$

From this, we obtain the relative permittivity for each orientation:

$$\varepsilon_i^*(\omega) = \varepsilon_m\left(1 + 3\phi C_i^*(\omega)\right) - j\frac{3\phi K_m}{\omega\varepsilon_0}\left(C_i^*(\omega) - C_i^*(\omega = 0)\right), \quad i \equiv \parallel, \perp \qquad [S.19]$$

and, for random orientation:

$$\left\langle \varepsilon^*(\omega) \right\rangle = \frac{\varepsilon_{\parallel}^*(\omega) + 2\varepsilon_{\perp}^*(\omega)}{3} \qquad [S.20]$$

3.2. Electrophoretic mobility

Considering the linearity of the electrophoresis problem, the (electrophoretic) velocity $\mathbf{v}_e$ can be written in terms of mobilities corresponding to both orientations:

$$\begin{aligned} \mathbf{v}_e &= u_{e\parallel}\mathbf{E}\cdot\hat{\mathbf{e}}_{\parallel}\hat{\mathbf{e}}_{\parallel} + u_{e\perp}(\mathbf{E} - \mathbf{E}\cdot\hat{\mathbf{e}}_{\parallel}\hat{\mathbf{e}}_{\parallel}) \\ \left\langle u_e \right\rangle &= \frac{u_{e\parallel} + 2u_{e\perp}}{3} \end{aligned} \qquad [S.21]$$

The important point here is to establish the relationship with the dipole coefficient. Hydrodynamic effects must also be taken into account, so that the Helmholtz-Smoluchowski equation must be modified as follows:[17]

$$u_{e,i} = \frac{\varepsilon_m\varepsilon_0}{\eta}\zeta f_{1,i}\cdot f_{2,i} \qquad [S.22]$$

where $f_{1,i}$ takes into account the particle inertia and $f_{2,i}$ measures the effect of EDL polarization. The former can be written, for whatever EDL processes, in terms of the drag coefficient $D_{H,i}$ and the added mass $M_{a,i}$[9,18]. Their expressions can be found in Ref.[18]. Concerning the second function, it was first evaluated by Loewenberg and O'Brien[9, 19, 20, 21] for the case $\kappa l_{\min} >> 1$, with $l_{\min}$ the minimum dimension of the spheroid (see Ref.[22, 23, 24] for an alternative derivation):

$$f_{2,i} = (1 - L_i) - 3L_i(1 - L_i)C_i^* \qquad [S.23]$$

Here L_i are the depolarization factors of the oblate spheroid:

$$L_{\square} = \frac{1}{1-r^2} - \frac{r}{(1-r^2)^{3/2}} \cos^{-1} r$$
$$L_{\perp} = \frac{1-L_{\square}}{2} \qquad [S.24]$$
$$(r = a/b)$$

3.3. The induced dipole coefficient for a spheroidal particle

Contrary to the case of spheres, the system of partial differential equations describing the electrokinetics of spheroids is not separable, so no analytical solution is available[25]. Some approximate models can be used though, as briefly mentioned below.

In the approximation of thin double layers, Dukhin and Shilov[26, 27] showed that the MWO relaxation could be described on the basis of the assumption of uniform field inside the spheroid and a combination of uniform and dipolar fields outside. A Debye-like relaxation of the dipole coefficient is found, given by:

$$C^*_{MWO,i}(\omega) = C^{\infty}_{MWO,i} + \frac{C^0_{MWO,i} - C^{\infty}_{MWO,i}}{1 + j\omega\tau_{MWO,i}}$$
$$\tau_{MWO,i} = \varepsilon_0 \frac{(1-L_i)\varepsilon_m + L_i\varepsilon_p}{(1-L_i)K_m + L_i K_{p,i}}$$
$$C^{\infty}_{MWO,i} = \frac{\varepsilon_p - \varepsilon_m}{3\left(\varepsilon_m + \left(\varepsilon_p - \varepsilon_m\right)L_i\right)} \qquad [S.25]$$
$$C^0_{MWO,i} = \frac{K_{p,i} - K_m}{3\left(K_m + \left(K_{p,i} - K_m\right)L_i\right)}$$

These expressions are valid if an effective complex conductivity is assigned to the spheroid for each orientation:

$$K^*_{p,i} = K_{p,i} + j\omega\varepsilon_0\varepsilon_p \qquad [S.26]$$

where the surface conductivity K^{σ} is related to the effective conductivities $K_{p,i}$ as follows:

$$\begin{aligned} K_{p,i} &= K^{\sigma} g_i \\ g_{\parallel} &= \frac{3a}{2bh}\left(\frac{2b^2-a^2}{h^2}\ln\frac{h+b}{a}-\frac{b}{h}\right) \\ g_{\perp} &= \frac{3a}{2bh}\left(\frac{b(2b^2-a^2)}{2h^3}-\frac{a^4}{2h^4}\ln\frac{h+b}{a}\right) \\ h &\equiv \sqrt{b^2-a^2} \end{aligned} \qquad [S.27]$$

In the low-frequency (α-relaxation) regime, the analysis of the concentration polarization is solved by considering separately the parallel and perpendicular orientations, distinguishing two characteristic diffusion lengths. According to Grosse and Shilov[28], the low-frequency dielectric increments read:

$$\begin{aligned} \delta\varepsilon_i'(0) &= \frac{3\varepsilon_m\kappa^2}{16\pi ab^2}\left(\gamma_i^+-\gamma_i^-\right)^2 I_i \\ \gamma_i^{\pm} &= \frac{ab^2}{3}\frac{K_{p,i}^{\pm}-K_m/2}{K_m/2+\left(K_{p,i}^{\pm}-K_m/2\right)L_i} \\ I_{\parallel} &= \frac{12\pi}{5h^6}\left(-a^3b^2\operatorname{arcot}^2\frac{a}{h}+hb^2(a^2+b^2)\operatorname{arcot}\frac{a}{h}-ah^2(h^2+b^2)\right) \\ I_{\perp} &= \frac{3\pi}{5h^6}\left(-ab^4\arccos^2\frac{a}{b}+2h(a^4+b^4)\arccos\frac{a}{b}-ah^2(3a^2-2b^2)\right) \end{aligned} \qquad [S.28]$$

The α-relaxation frequencies for the two orientations are given below. Contrary to the case of prolate spheroids, it is likely that the two characteristic frequencies are similar, and mainly controlled by the larger semiaxis: whatever the orientation, ions will not find a diffusion distance of the order to the smaller particle dimension:

$$\omega_\alpha^i = \frac{16\pi ab^2\left(C_{i,\alpha}(\infty) - C_{i,\alpha}(0)\right)}{\kappa^2\left(\gamma_i^+ - \gamma_i^-\right)^2 I_i}\frac{K_m}{\varepsilon_m}$$

$$C_{i,\alpha}(0) = \frac{\gamma_i^+ + \gamma_i^-}{2ab^2} \qquad [S.29]$$

$$C_{i,\alpha}(\infty) = \frac{K_{p,i} - K_m}{3\left(K + \left(K_{p,i} - K_m\right)L^i\right)}$$

Once the experimental dielectric dispersion (DD) spectrum is found, the model can be used for estimating both the zeta potential and the large semiaxis*b* (radius of the equator of the oblate spheroid). Our experimental data of $\varepsilon_D''(\omega)$ are fitted to the logarithmic derivative of the empirical Cole-Cole function

$$\Delta\varepsilon^*(\omega) = \frac{\Delta\varepsilon'(0)}{1 + \left(i\omega/\omega_{\max}\right)^{1-\alpha}} \qquad [S.30]$$

and the values of the low frequency dielectric increment $\Delta\varepsilon'(0)$ and of the frequency $\omega_{\max}$ (corresponding to the maximum in the $\varepsilon_D''(\omega)$ spectrum) are extracted. In the case of the dielectric dispersion of suspensions of spheres, the relationship between $\omega_{\max}$ and the α-relaxation frequency ω_α can be obtained by assuming that the actual relaxation is a Vogel-Pauly[29] function, from which ω_α can be directly obtained. It is found that $\omega_{\max}$ is systematically lower than ω_α by a factor around 0.4 depending on the value of $\Delta\varepsilon'(0)$. Because there is no theoretical treatment for spheroids, we may assume that the same relationship holds. Finally, Grosse et al.'s model[30] is used for obtaining the surface conductivity and the particle diameter 2*b*, by assuming that the low-frequency dielectric increment can be associated to a random orientation of the particles, as in eq [S.20]:

$$\Delta\varepsilon'(0) = \frac{\Delta\varepsilon_{\square}'(0) + 2\Delta\varepsilon_{\perp}'(0)}{3} \qquad [S.31]$$

and also that the experimental ω_α is a similar average of $\omega_\alpha^{||}$ and $\omega_\alpha^{\perp}$.

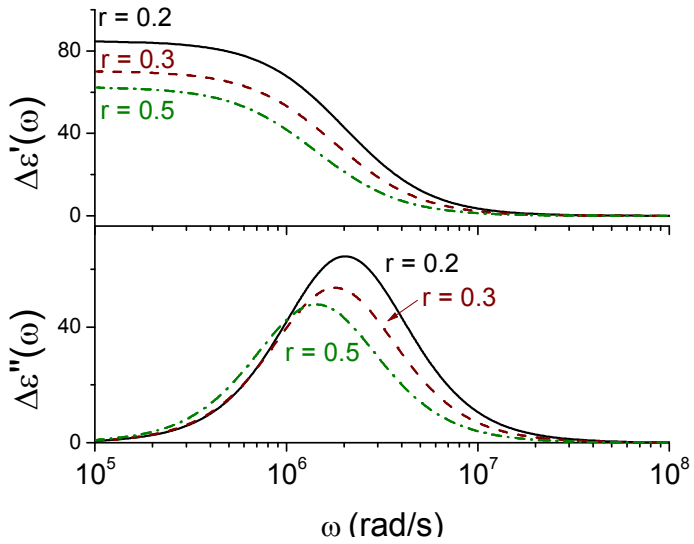

Figure S5: Real (top) and imaginary (bottom) components of the dielectric increment of suspensions of oblate spheroids as a function of frequency, for different values of the axial ratio $r = a/b$. In all cases, b = 200 nm; ζ = 100 mV; volume fraction of solids ϕ = 0.02; KCl 1 mM.

Figure S5 confirms the expected results concerning the location of the relaxation frequency. It shows that increasing the eccentricity of the particle (decreasing r) shifts the relaxation frequency towards slightly higher values (giving more chance to short diffusion lengths to show up), and produces larger dielectric increments at low frequencies. However, the fact that the relaxation extends over a frequency

decadecentered at 2-4×10^5 Hz indicates that the small and large semiaxes contributions are not well separated in frequency.

4. Correction of electrode polarization in DD measurements

As mentioned in the manuscript, the logarithmic derivative method was used for minimizing the effect of electrode polarization. In this section we illustrate the method by applying it to some examples.

We reproduce in Figure S6 the raw data obtained at pH 4 and pH 5 with KCl 0.5 and 1 mM. The electrode polarization manifests itself in the strong rise of the apparent logarithmic derivative at low frequency. Note that the electrode polarization has the same contribution at both pHs, as it is expected since they have the same ionic strength. In a log-log plot, this corresponds to a linear portion of the spectra that can be fitted and subtracted from the raw data as shown in Figure S7. In this figure we show how the DD data are treated to minimize the contribution of electrode polarization and finally get what can be considered the "true" relaxations. For this purpose we fit the low frequency part of the spectra, where only electrode polarization contributes, to a power law (lines in Figure S7), and then this curve is subtracted from the raw data. This example serves to illustrate the differences between pH 4 and 5, namely, the existence of a second relaxation phenomenon at low frequency which appears at pH 4, but is not observed at pH 5.

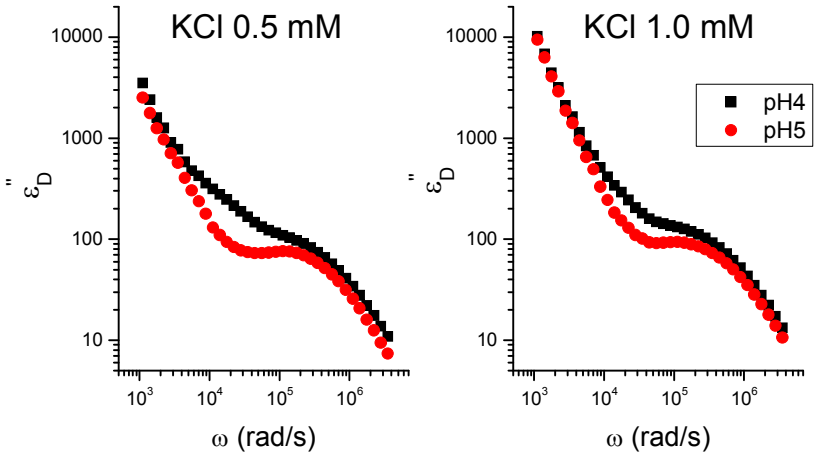

Figure S6. Raw data of the logarithmic derivative of the real component of the relative permittivity as a function of the frequency, for a suspension 2% volume fraction of gibbsite particles and the pH and ionic strength indicates.

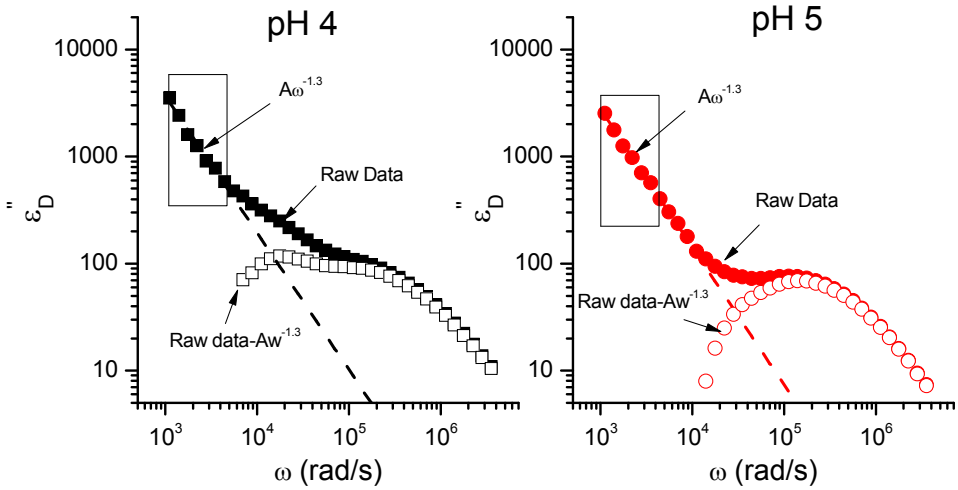

Figure S7. Raw data of the logarithmic derivative of the real part of the dielectric permittivity (full symbols), electrode polarization fitting lines (dashed lines), and corrected DD data (open symbols) as a function of frequency. In all cases thevolume fraction of gibbsite particles is 2%. pH values as indicated and KCl 0.5 mM.

REFERENCES

(1) O'Brien, R. W.; Ward, D. N. The electrophoresis of a spheroid with a thin double-layer. *J. Colloid Interface Sci.* **1988**, *121*, 402-413.

(2) Grosse, C. Relaxation Mechanisms of Homogeneous Particles and Cells Suspended in Aqueous Electrolyte Solutions. In *Interfacial electrokinetics and electrophoresis.*, Delgado, A. V., Ed.; Marcel Dekker: New York, 2002; Vol. 106, p 277.

(3) Dukhin, S. S.; Shilov, V. N. *Dielectric phenomena and the double layer in disperse systems and polyelectrolytes*; Jerusalem Keter Publishing: Jerusalem, 1974. p 192.

(4) Shilov, V. N.; Delgado, A. V.; González-Caballero, E.; Horno, J.; López-García, J. J.; Grosse, C. Polarization of the electrical double layer. Time evolution after application of an electric field. *J. Colloid Interface Sci.* **2000**, *232*, 141-148.

(5) Lyklema, J. *Fundamentals of Interface and Colloid Science*; Elsevier: Amsterdam, 2005; Vol. IV.

(6) Jiménez, M. L.; Arroyo, F. J.; Carrique, F.; Delgado, A. V. Surface conductivity of colloidal particles: Experimental assessment of its contributions. *J. Colloid Interface Sci.* **2007**, *316*, 836-843.

(7) Overbeek, J. T. G. On smoluchowski equation for the electrophoresis of colloidal particles. *Philips Research Reports* **1946**, *1*, 315-319.

(8) O'Brien, R. W.; White, L. R. Electrophoretic mobility of a spherical colloidal particle. *J. Chem. Soc. Faraday Trans. II* **1978**, *74*, 1607-1626.

(9) Loewenberg, M.; O'Brien, R. W. The dynamic mobility of nonspherical particles. *J. Colloid Interface Sci.* **1992**, *150*, 158-168.

(10) Ohshima, H. Dynamic electrophoretic mobility of spherical colloidal particles in concentrated suspensions. *J. Colloid Interface Sci.* **1997**, *195*, 137-148.

(11) Rasmusson, M.; Rowlands, W.; O'Brien, R. W.; Hunter, R. J. The dynamic mobility and dielectric response of sodium bentonite. *J. Colloid Interface Sci.* **1997**, *189*, 92-100.

(12) Dukhin, A. S.; Shilov, V.; Borkovskaya, Y. Dynamic electrophoretic mobility in concentrated dispersed systems. Cell model. *Langmuir* **1999**, *15*, 3452-3457.

(13) Arroyo, F. J.; Carrique, F.; Ahualli, S.; Delgado, A. V. Dynamic mobility of concentrated suspensions. Comparison between different calculations. *Phys. Chem. Chem. Phys.* **2004**, *6*, 1446-1452.

(14) Delgado, A. V.; Ahualli, S.; Arroyo, F. J.; Carrique, F. Dynamic electrophoretic mobility of concentrated suspensions - Comparison between experimental data and theoretical predictions. *Colloids Surf A-Physicochem. Eng. Aspects* **2005**, *267*, 95-102.

(15) Ahualli, S.; Arroyo, F.; Carrique, F.; Jiménez, M.L.; Delgado, A.; IEEE. Electroacoustic and dielectric dispersion of concentrated colloidal suspensions. *ICDL: 2005 IEEE International Conference on Dielectric Liquids* **2005**, 49-52.

(16) O'Brien, R. W. The electroacoustic equations for a colloidal suspension. *J. Fluid Mech.* **1990**, *212*, 81-93.

(17) Rica, R. A.; Jiménez, M. L.; Delgado, A. V. Dynamic Mobility of Rodlike Goethite Particles. *Langmuir* **2009**, *25*, 10587-10594.

(18) Lawrence, C. J.; Weinbaum, S. The unsteady force on a body at low Reynolds numbe. The axisymmetric motion of a spheroid. *J. Fluid Mech.* **1988**, *189*, 463-489.

(19) Loewenberg, M. Stokes resistance, added mass, and Basset force for arbitrarily oriented, finite-length cylinders. *Phys. Fluids A-Fluid Mech.* **1993**, *5*, 765-767.

(20) Loewenberg, M. The unsteady stokes resistance of arbitrarily oriented, finite-length cylinders. *Phys. Fluids A-Fluid Mech.***1993**, *5*, 3004-3006.

(21) Loewenberg, M. Unsteady electrophoretic motion of a nonspherical colloidal particle in an oscillating electric-field. *J. Fluid Mech.* **1994**, *278*, 149-174.

(22) Chassagne, C.; Bedeaux, D. The dielectric response of a colloidal spheroid. *J. Colloid Interface Sci.* **2008**, *326*, 240-253.

(23) Chassagne, C.; Mietta, F.; Winterwerp, J. C. Electrokinetic study of kaolinite suspensions. *J. Colloid Interface Sci.* **2009**, *336*, 352-359.

(24) Chassagne, C. Dielectric Response of a Charged Prolate Spheroid in an Electrolyte Solution. *Int. J. Thermophys.* **2013**, *34*, 1239-1254.

(25) Fixman, M. A macroion electrokinetics algorithm. *J. Chem. Phys.* **2006**, *124*.

(26) Derjaguin, B. V.; Dukhin, S. S.; Shilov, V. N. Kinetic aspects of electrochemistry of disperse systems. 1. Introduction. *Adv. Colloid Interface Sci.* **1980**, *13*, 141-152.

(27) Dukhin, S. S.; Shilov, V. N. Kinetic aspects of electrochemistry of disperse systems. 2. Induced dipole-moment and the nonequilibrium double-layer of a colloid particle. *Adv. Colloid Interface Sci.* **1980**, *13*, 153-195.

(28) Grosse, C.; Shilov, V. N. Calculation of the static permittivity of suspensions from the stored energy. *J. Colloid Interface Sci.* **1997**, *193*, 178-182.

(29) Vogel, E.; Pauly, H. Dynamic dipole polarizability of a dielectric sphere in an electrolyte *J. Chem. Phys.* **1988**, *89*, 3823-3829.

(30) Grosse, C.; Pedrosa, S.; Shilov, V. N. Calculation of the dielectric increment and characteristic time of the LFDD in colloidal suspensions of spheroidal particles. *J. Colloid Interface Sci.* **1999**, *220*, 31-41.